

## Threshold criteria for real time RF monitoring in 7T parallel transmit system

B. Gagoski<sup>1</sup>, H. Bhat<sup>2</sup>, P. Hoecht<sup>2</sup>, K. Makhoul<sup>3,4</sup>, U. Fontius<sup>5</sup>, J. Pfeuffer<sup>5</sup>, F. Schmitt<sup>5</sup>, M. Hamm<sup>2</sup>, J. Lee<sup>1</sup>, K. Setsompop<sup>3,4</sup>, L. L. Wald<sup>3,6</sup>, and E. Adalsteinsson<sup>1,6</sup>

<sup>1</sup>Electrical Engineering and Computer Science, Massachusetts Institute of Technology, Cambridge, MA, United States, <sup>2</sup>Siemens Healthcare, Charlestown, MA, United States, <sup>3</sup>A.A. Martinos Center for Biomedical Imaging, Department of Radiology, Massachusetts General Hospital, Charlestown, MA, United States, <sup>4</sup>Harvard Medical School, Boston, MA, United States, <sup>5</sup>Siemens Healthcare, Erlangen, Germany, <sup>6</sup>Harvard-MIT Division of Health Sciences and Technology, MIT, Cambridge, MA, United States

**Introduction:** Parallel RF transmission (pTx) provides spatial and temporal degrees of freedom to shorten the duration of spatially tailored excitation pulses compared to single-channel excitations. Monitoring and management of the local specific absorption rate (SAR) is critical to routine deployment of pTx systems for ultra-high field *in vivo* imaging. Local SAR distribution due to a given pTx RF pulse can be estimated with numerical modeling [1] and either the pulse design or sequence timing parameters can be adjusted to adhere to limits on local or global SAR. However, to guard against run-time deviations in pTx RF waveforms that may result in violation of SAR limits, real-time RF waveform monitoring serves an important role. Real-time RF monitoring of the forward and reflected power to each channel through pickup loops [2] or directional couplers (DiCos) [3] provides the means to detect deviations in multichannel pTx RF waveforms from their intended signals.

In this work we investigated subject-to-subject variation in excitation coil array monitoring parameters and use these findings to propose threshold criteria to detect a mismatch between ideal and observed RF signals. Calibration of the cut-off values needed in the threshold algorithm was done empirically by monitoring the RF signals in 15 *in vivo* measurements. The performance of the proposed algorithm was then tested for different types of RF pulses in undisturbed and purposely disturbed acquisitions. Once the given proposed threshold was exceeded, the measurement was successfully stopped in real time.

**Methods:** Eight DiCos were used to measure the forward and reflected power to an 8-channel transmit coil array for a MAGNETOM 7T (Siemens Healthcare, Erlangen, Germany) with an 8-channel prototype pTx system. A dedicated calibration sequence, with scan time of less than 10s, estimated the complex-valued 8x8 coupling matrices that transform the transmitted power waveform  $p_i(t)$  for each channel,  $i$ , set by the digital pulse waveform to the forward or reflected power at each 50Ohm matched coil. Designating these 8x8 coupling matrices,  $\alpha_{FWD}$  and  $\alpha_{REF}$  [4] for the forward and reflected measurements, the values of these alpha matrices, particularly those of  $\alpha_{REF}$ , vary from one subject to the next due to modulation of the array couplings by loading differences. In order to quantify this variability, we collected  $\alpha_{FWD}$  and  $\alpha_{REF}$  for each of the 15 different subjects who were asked to position, remove and then re-position their head in the array three times. We analyzed the calibration matrix for the delivered power,  $\alpha = (\alpha_{FWD} - \alpha_{REF})$ . Defining  $\alpha_{mean\_archive}$  as the mean among all the  $\alpha$ 's, we calculated the maximum error vector  $\epsilon_{max\_a}$ , such that  $\epsilon_{max\_a}[n] = \max[(\alpha_n - \alpha_{mean\_archive})/(\alpha_{mean\_archive})]$ , for  $n = [1...45]$ . Reshaping  $\epsilon_{max\_a}$  to [3x15] matrix (3 measurements per head; 15 heads), and taking the mean along the first direction, gives the mean maximum error for each head.

Every new pTx session starts with an acquisition of  $\alpha_{FWD\_curr}$  and  $\alpha_{REF\_curr}$  for the current subject. Then, for  $\alpha_{curr} = (\alpha_{FWD\_curr} - \alpha_{REF\_curr})$ , we calculate the maximum error relative to  $\alpha_{mean\_archive}$ , i.e.  $\epsilon_{max\_curr} = \max[(\alpha_{curr} - \alpha_{mean\_archive})/(\alpha_{mean\_archive})]$ . If  $\epsilon_{max\_curr} > \epsilon_{max}$ , we question the state of our hardware and abort the session. If  $\epsilon_{max\_curr} < \epsilon_{max}$ , we proceed with our experiments.

For a given set of pTx RF pulses  $b(t)$ , played at a maximum transmit voltage,  $TX_{vol}$ , the forward and reflected RF signals from the DiCos ( $b_{m\_FWD}(t)$  and  $b_{m\_REF}(t)$ , respectively) are compared against  $b_{e\_FWD}(t) = TX_{vol} \cdot b(t) \cdot \alpha_{FWD}$  and  $b_{e\_REF}(t) = TX_{vol} \cdot b(t) \cdot \alpha_{REF}$ , by defining the normalized complex error matrix  $\epsilon = [(b_{m\_FWD}(t) - b_{m\_REF}(t)) - (b_{e\_FWD}(t) - b_{e\_REF}(t))] / (b_{e\_FWD}(t) - b_{e\_REF}(t))$ . Then, the proposed threshold algorithm does the following: 1. Finds  $v_{ind\_e}$ , the vector of indexes of all RF samples in  $\epsilon$  that exceed the empirically obtained  $\epsilon_{max} = 5\%$ ; 2. For the RF samples at the indexes  $v_{ind\_e}$ , assumes the worst case scenario when all the E fields sum constructively, so the maximum 10g-avg local SAR,  $SAR_{10g\_local\_curr}$  is further derated by a local SAR term  $SAR_{10g\_local\_e} = P(v_{ind\_e}) / r_{worst\_case} / m_{head}$  due to the "erroneous" samples. Here,  $P(v_{ind\_e}) = \sum b(v_{ind\_e})^2 / 50\Omega$ ,  $r_{worst\_case}$  is the worst case  $SAR_{10g\_local} / SAR_{global}$  for the array and is typically  $\sim 60$  [5] and  $m_{head} = 4kg$  is the mass of the head; and 3. Stops the measurement in real time if the minimum TR calculated based on new SAR estimate (using the worst case scenario for time points for which  $\epsilon > 5\%$ ), is longer than the TR being used.

**Results and Discussion:** In the multi-subject study, it was found that  $\epsilon_{max} = 5\%$ , which was considered to be the upper limit of the range of variability present in our monitoring system. The feasibility of the proposed threshold criteria was then tested on pTx excitations using spokes and spiral trajectories. Table 1 presents the performance of the RF monitoring for several excitations by showing the values for  $TX_{vol}$ ,  $SAR_{10g\_local\_e}$ , the percent increase of  $SAR_{10g\_local\_curr}$  due to  $SAR_{10g\_local\_e}$  (and hence the minimum TR), and the percentage of RF samples with monitored error values greater than  $\epsilon_{max} = 5\%$  (in the TR with maximum length  $v_{ind\_e}$ ). Two acquisitions were purposely disturbed by adding 0.25m of extra cable on TX#7 to change its phase ("spokes\_pulse\_disturbed"), and by putting a small titanium piece next to the TX-coil element #4 to change its tuning ("2D\_spiral\_pulse\_disturbed"). As expected, for these cases, the threshold criteria triggered acquisition stop. For the other excitation shown, the match was good and well within the target error criterion over all the TRs played. Fig1 shows overlay plot of  $b_{m\_FRW}(t) - b_{m\_REF}(t)$  (blue) and  $b_{e\_FRW}(t) - b_{e\_REF}(t)$  (red) for the real part of "2D\_spiral\_pulse" (for TX2), and the real and imaginary parts for TX5 to TX8 of "Spokes\_pulse\_disturbed".

**Conclusion:** We used 15 subjects with three repeated calibration acquisitions

to evaluate the intrinsic subject-induced variability in a pTx RF monitoring system with directional couplers. The calibrated cut-off values (5%) were applied in a threshold algorithm, which incorporated worst-case local SAR criteria to derate the applied power based on worst-case local SAR calculations during periods where the waveforms deviated from that expected. The algorithm was tested for two types of RF pulses in disturbed and undistorted conditions, and was shown to perform as expected.

**Support:** NIH: R01EB007942, R01EB006847, NCRR P41RR14075; Siemens Healthcare, Erlangen; Siemens Medical Solutions USA; Siemens-MIT Alliance. **Disclaimer:** The concepts and information presented in this paper are based on research and are not commercially available.

**References:** [1] Zelinski A., et al., *JMRI*, 28, p1005-18, 2008; [2] Graesslin I. et al, *Proc. to 15<sup>th</sup> ISMRM*, 2007, p 1086. [3] Alon L. et al, *Proc. to 18<sup>th</sup> ISMRM*, 2010, p 780. [4] Gagoski B. et al, *Proc. to 18<sup>th</sup> ISMRM*, 2010, p 781. [5] Collins C.M. et al, *Proc. to 15<sup>th</sup> ISMRM*, 2007, p 1092.

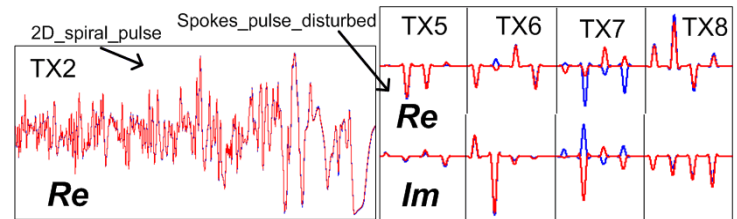


Fig 1: Overlay of  $b_{m\_FRW}(t) - b_{m\_REF}(t)$  (blue) and  $b_{e\_FRW}(t) - b_{e\_REF}(t)$  (red) for "2D\_spiral\_pulse" and "Spokes\_pulse\_disturbed" acquisitions

	$TX_{vol}$	$SAR_{10g\_local\_e}$	% $\uparrow$ wrt $SAR_{10g\_local\_curr}$	% samples $> \epsilon_{max}$	Scan stopped?
Spokes_pulse	100 V	0 W/kg	0%	0%	NO
2D_spiral_pulse	160 V	1.44 W/kg	4.6%	2.03%	NO
Spokes_pulse_disturbed	180 V	53.35 W/kg	590.1%	25.38%	YES
2D_spiral_pulse_disturbed	180 V	12.47 W/kg	145.2%	14.17%	YES

Table 1: Evaluating the performance of the threshold criteria for four pTx excitations (see text)